AIP | Applied Physics Letters

Shell-thickness-dependent photoinduced electron transfer from CuInS2/ZnS quantum dots to TiO2 films

Jianhui Sun, Jialong Zhao, and Yasuaki Masumoto

Citation: Appl. Phys. Lett. **102**, 053119 (2013); doi: 10.1063/1.4790603
View online: http://dx.doi.org/10.1063/1.4790603
View Table of Contents: http://apl.aip.org/resource/1/APPLAB/v102/i5
Published by the American Institute of Physics.

Shell-thickness-dependent photoinduced electron transfer from $CuInS_2$/ZnS quantum dots to TiO_2 films

Jianhui Sun,[1,2,3] Jialong Zhao,[2,a)] and Yasuaki Masumoto[1,b)]
[1]*Institute of Physics, University of Tsukuba, Tsukuba 305-8571, Japan*
[2]*State Key Laboratory of Luminescence and Applications, Changchun Institute of Optics, Fine Mechanics and Physics, Chinese Academy of Sciences, Changchun 130033, China*
[3]*University of Chinese Academy of Sciences, Beijing 100039, China*

(Received 6 December 2012; accepted 21 January 2013; published online 6 February 2013)

We demonstrate the electron transfer (ET) processes from $CuInS_2$/ZnS core/shell quantum dots (QDs) into porous anatase TiO_2 films by time-resolved photoluminescence spectroscopy. The rate and efficiency of ET can be controlled by changing the core diameter and the shell thickness. It is found that the ET rates decrease exponentially at the decay constants of 1.1 and 1.4 nm^{-1} with increasing ZnS shell thickness for core diameters of 2.5 and 4.0 nm, respectively, in agreement with the electron tunneling model. This shows that optimized ET efficiency and QD stability can be realized by controlling the shell thickness. © *2013 American Institute of Physics*.
[http://dx.doi.org/10.1063/1.4790603]

Quantum dots (QDs) have been considered as a revolutionizing material in next-generation photovoltaics (PVs)[1,2] because of their size-dependent properties, flexible solution-processing, and higher photostability compared to traditional organic dyes. Efficient electron transfer (ET) from QDs to external electrodes is a key factor to achieve high power-conversion-efficiency in PVs. From Marcus theory,[3] the ET rate is determined by the electronic coupling strength (H_{DA}), the total reorganization energy (λ), and the driving force energy (ΔG). In donor-acceptor hybrid systems of CdSe,[4–6] CdS,[7] and PbS QDs[8] tethered to TiO_2 or ZnO, the effects of above three parameters on the ET dynamics have been explored widely. The photoelectrochemical response has been tuned via the size control of CdSe QDs to obtain the maximum photoconversion efficiency in QD-sensitized solar cells.[6] It is well known that overcoating CdSe QDs with wide band-gap shell materials, such as ZnS, to form type I core/shell structures can greatly enhance their photo- and thermal-stability[9] and efficiency[10] in QD-sensitized solar cells. Bulk $CuInS_2$ has a direct bandgap of 1.53 eV, which is well matched with the optimal spectral range for photovoltaic applications, resulting in Cd-free solar harvesters in solar cells. The band gap of $CuInS_2$ QDs can be tuned not only by controlling their size[11,12] and stoichiometry[13,14] but also by introducing other elements such as Zn.[15–18] Therefore, they are considered to be alternative low-toxicity materials as solar harvesters for the solution-processed PVs.[19] We need to fully understand the extraction efficiency of photogenerated charges from $CuInS_2$ QDs to the external electrodes, such as TiO_2, by controlling their size and surface structures for better performances of the PVs.

Here, we demonstrate efficient electron injection from $CuInS_2$ core and $CuInS_2$/ZnS core/shell QDs to the porous anatase TiO_2 films by using steady-state and time-resolved photoluminescence (PL) spectroscopy. The relevant energy levels of $CuInS_2$ QDs are obtained by cyclic voltammetry (CV) measurements, which is in accordance with the values calculated by the effective mass approximation (EMA).[12] The lowest unoccupied molecular orbital (LUMO) level in $CuInS_2$ QDs is above that of the TiO_2 films, resulting in the efficient electron injection into TiO_2 films from $CuInS_2$ QDs. The effect of the core diameter and the ZnS shell thickness on the ET rate and efficiency is studied in detail. We make the tunneling calculation to describe the ET rate as a function of the shell thickness and to understand the ET rate and efficiency in the QD/TiO_2 system.

The $CuInS_2$ core and $CuInS_2$/ZnS core/shell QDs were synthesized by means of the wet chemical method.[13] Transmission electron microscopy (TEM) images of the QDs are shown in the inset of Fig. 1(a), which determine the diameter of three samples of $CuInS_2$ core QDs to be 2.5, 3.3, and 4.0 nm, respectively. Furthermore, the $CuInS_2$ core QDs were coated with a ZnS shell to form the $CuInS_2$/ZnS core/shell QDs by means of a successive ionic layer adsorption and reaction (SILAR) methods.[13] The size and the size distribution histogram of the $CuInS_2$/ZnS core/shell QDs determined by TEM are shown in supplementary material.[20] The TiO_2 and ZrO_2 metallic oxide electrodes used in this work were fabricated by the same method reported before.[21] As for the QDs-sensitization, metallic oxide electrodes were tethered 3-mercaptopropionic acid (MPA) first and then immersed in QDs in toluene.[6] Time-resolved PL was measured by means of a time-correlated single photon counting (TCSPC) system with a visible photomultiplier and a 70 ps pulsed diode laser emitting at 375 nm. Time resolution of the TCSPC system was about 1 ns.

The absorption and PL spectra of synthesized $CuInS_2$ core QDs are shown in Fig. 1(a). The absorption edge gradually shifts toward longer wavelength with increasing the diameter of the QDs, in consistent with quantum confinement effect. Emission peaks of the QDs exhibit a large Stokes shift of about 300 meV from their corresponding optical band gaps, indicating that the radiative transition does not come from excitonic recombination.[11–14]

[a)]Electronic mail: zhaojl@ciomp.ac.cn.
[b)]Electronic mail: shoichi@sakura.cc.tsukuba.ac.jp. URL: http://www.sakura.tsukuba.ac.jp/~masumoto.

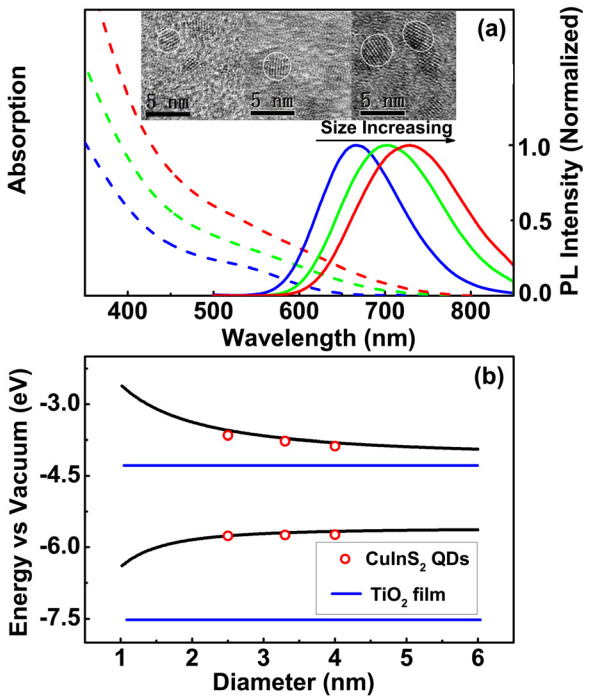

FIG. 1. (a) Steady-state PL and absorption spectra of $CuInS_2$ core QDs with diameters of 2.5 (blue), 3.3 (green), and 4.0 nm (red), respectively, in toluene and the corresponding high-resolution TEM image from left to right. The scale bar is 5 nm; (b) The LUMO and HOMO levels of $CuInS_2$ QDs shown by red circles were measured by CV. Black lines represent LUMO and HOMO levels of the $CuInS_2$ QDs calculated in EMA. Blue lines represent the LUMO and HOMO levels of the TiO_2 film measured by CV and optical absorption.

The LUMO and the highest occupied molecular orbital (HOMO) energy levels of the $CuInS_2$ core QDs were obtained from a CV method. The resulting energy levels shown in Fig. 1(b) by red circles are consistent with the energy levels calculated in EMA with a finite-depth well,[12] where LUMO and HOMO levels of bulk $CuInS_2$ are assumed to be -4.1 eV and -5.6 eV,[22] respectively. The effective masses of electrons and holes are $0.16m_0$ and $1.30m_0$, respectively, where the m_0 is the electron mass in vacuum.[10] The LUMO level of the porous anatase TiO_2 film obtained from the CV method is located at -4.21 eV, which is much lower than the LUMO level of -3.88 eV for the largest $CuInS_2$ core QDs. Therefore, the ET from the QDs to the porous anatase TiO_2 films is energetically allowable. According to the Marcus theory, the ET between two states is dominated by ΔG.[3,4] In the case of electron injection into TiO_2, the ΔG is the difference between the lowest quantum electron level of the QDs and the LUMO level of TiO_2. As the ΔG between acceptor and donor systems increases, the ET rate increases and reaches a maximum when the ΔG is equal to the reorganization energy.

PL decay curves of the $CuInS_2$ core QDs 2.5, 3.3, and 4.0 nm in average diameter deposited on TiO_2 and ZrO_2 films are shown in Fig. 2. From the PL dynamics of the $CuInS_2$ core QDs, the fast decay comes from nonradiative surface-traps and the long lifetime contribution is ascribed to the internal defect state emission. Recently, the long lifetime emission was suggested to originate from the recombination from an electron quantum state to a localized hole state.[11]

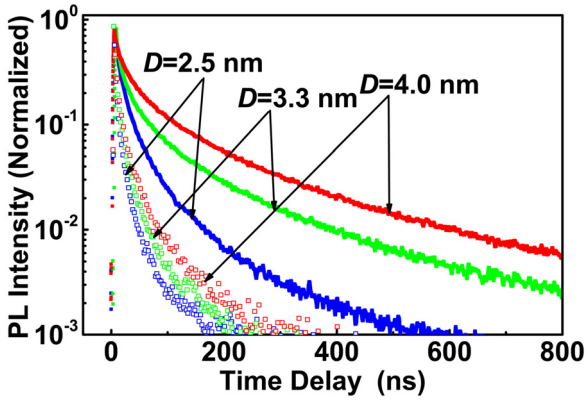

FIG. 2. PL decay curves of $CuInS_2$ core QDs deposited on the ZrO_2 (solid dots) and TiO_2 films (empty dots).

The LUMO level of the ZrO_2 film was obtained to be -3.17 eV, which is even higher than the LUMO level of -3.65 eV in the smallest $CuInS_2$ core QDs. Therefore, the ET from $CuInS_2$ QDs to ZrO_2 is energetically unfavorable, and thus the observed PL decay curves in this system can be used as a reference. The significant shortening in the PL decays of $CuInS_2$ core QDs is clearly observed. This suggests that the ET adds another decay channel to the excited states of the QDs. To calculate the ET rate, we assume that the average PL lifetimes of the QDs on TiO_2 and ZrO_2 films are given by $\tau_{QD-TiO_2} = 1/(k_R + k_{NR} + k_{ET})$ and $\tau_{QD-ZrO_2} = 1/(k_R + k_{NR})$, respectively, where k_R and k_{NR} are radiative and nonradiative decay rates for QDs, respectively.[4–6] The ET rate (k_{ET}) and efficiency (η_{ET}) can be calculated as: $k_{ET} = 1/\tau_{QD-TiO_2} - 1/\tau_{QD-ZrO_2}$ and $\eta_{ET} = 1 - \tau_{QD-TiO_2}/\tau_{QD-ZrO_2}$, respectively. The evaluated ET rates and efficiencies are summarized in Table I. The ET rate reaches 10^7 s^{-1} close to the rate in CdSe-TiO_2 donor-accepter systems.[4,6,24] The rate slightly increases with decreasing the core diameters of the $CuInS_2$ QDs, in consistent with the Marcus theory. However, the size dependence of the ET rate is clearly lower than that of CdSe QDs.[4] On the other hand, the ET efficiency shows the opposite trend. The maximum efficiency is obtained in the largest $CuInS_2$ QDs. It has been reported the ET process is impeded in QDs by the considerable amount of surface-localized trap states.[1,5] Considering that the luminescence of the $CuInS_2$ QDs is significantly reduced by the surface traps and that the PL lifetimes of $CuInS_2$ QDs in toluene are shortened with decreasing the diameters, we attribute the low ET efficiency in small $CuInS_2$ QDs to the relatively large amount of surface-localized states.

As known, the stability of bare QDs remains an issue due to photo-induced oxidation in photovoltaic devices.[5] We

TABLE I. The efficiency (η_{ET}) and rate (κ_{ET}) of ET from $CuInS_2$ QDs to the porous anatase TiO_2 film.

Diameters of $CuInS_2$ (nm)	κ_{ET} (10^7 s^{-1})	η_{ET} (%)
2.5	6.0	69
3.3	5.4	74
4.0	4.5	83

further investigated photoinduced ET into TiO_2 from $CuInS_2$/ZnS core/shell QDs. With increasing the ZnS shell thickness, the PL peak of the QDs slightly shifts to higher energy compared with the bare QDs, which is slightly different from the case of CdSe/ZnS core/shell QDs.[11,13] For $CuInS_2$/ZnS core/shell QDs, the surface coating by a ZnS shell involves an interdiffusion alloying process, perhaps resulting in formation of an inner alloying layer and etching of the $CuInS_2$ cores. However, we ignored the size change of the $CuInS_2$ core in order to facilitate the estimation of the ZnS shell thickness. As shown in Fig. 3, the PL lifetimes of the $CuInS_2$/ZnS core/shell QDs tethered onto the ZrO_2 films exhibit a significant increase with increasing the shell thickness, suggesting the improved passivation of surface defects in the QDs.

PL decay curves of the two series of $CuInS_2$/ZnS core/shell QDs 2.5 and 4.0 nm in core diameter tethered onto the TiO_2 films are shown in Fig. 3. It is expected that the ZnS shell acts as a tunneling barrier for ET from the photoexited $CuInS_2$ QDs to the TiO_2 film because the H_{DA} between $CuInS_2$ QDs and a TiO_2 film would be weakened with increasing the ZnS shell thickness. The ET rates for the two series of core/shell QDs plotted as a function of ZnS shell thickness are shown in Fig. 4. As we expected, the ET rate rapidly decreases with increasing the ZnS shell thickness. The decrease in the ET rate is considered to result from the weak electronic coupling between the TiO_2 films and the QDs with the increase of the ZnS shell thickness. Surprisingly, the ET efficiency slightly decreases with the increase of ZnS shell thickness. For example, the ET efficiency of QDs 2.5 nm in core diameter decreases from 65% for the 1.1 monolayer (ML) ZnS shell to 38% for the 3.2 ML ZnS shell. Despite the significant decrease in the ET rate in contrast

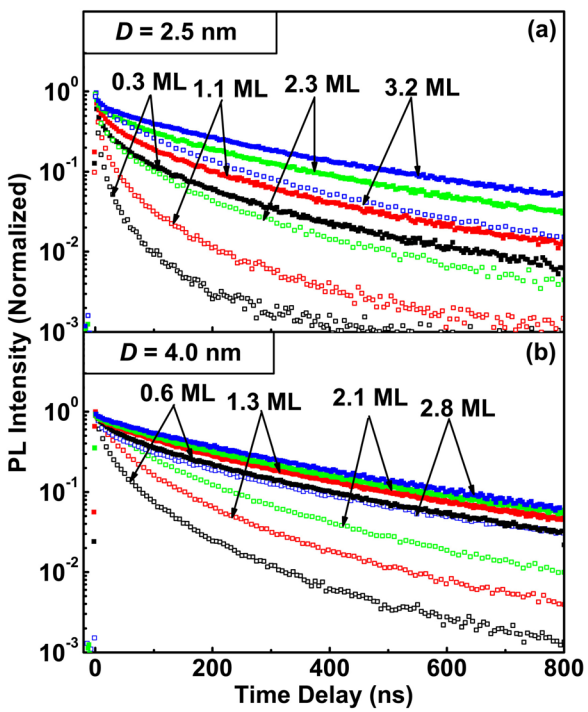

FIG. 3. PL decay curves of $CuInS_2$/ZnS core/shell QDs with various core diameters and the ZnS shell thicknesses deposited on the ZrO_2 (solid dots) and TiO_2 films (empty dots).

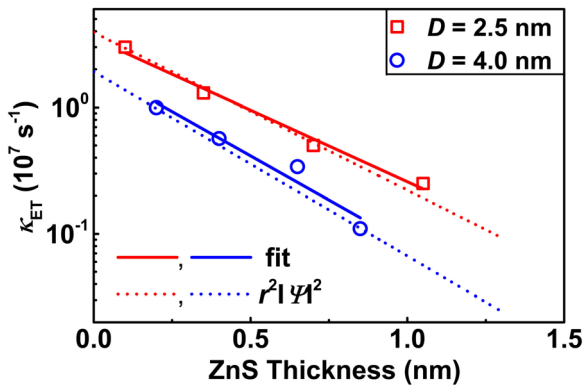

FIG. 4. Plots of ET rates of $CuInS_2$/ZnS core QDs with core diameters of $D = 2.5$ nm (red squares) and $D = 4.0$ nm (blue circles), respectively, as a function of ZnS shell thickness. The solid line represents the fit of the ET rate. The calculated electron densities at the ZnS surface as a function of ZnS shell thickness are shown by dashed lines. The electron densities lines were normalized to the fastest measured ET rates for comparison.

with that for the $CuInS_2$ core QDs, the $CuInS_2$/ZnS core/shell QDs exhibit only a slight reduction in ET efficiency with increasing the ZnS shell thickness. This is because a thin ZnS shell can effectively reduce the number of the traps as nonradiative recombination centers and results in efficient enhancement in the PL quantum efficiency.[11] This gives us a hint that how we can control the ET rate and the ET efficiency in such a donor-accepter system by controlling the QDs shell thickness to optimize the performance of the QD-based solar cells.

We assume the LUMO and HOMO levels of the $CuInS_2$ core remain unchanged for different thickness of the ZnS shell and ignore the intersphere distance between the $CuInS_2$/ZnS QDs and TiO_2 films.[24] The ET rates should be related to the thickness of the shell and could be described by the following expression:[5,23]

$$k(d) = k_0 e^{-\beta d}, \quad (1)$$

where d is the thickness of the ZnS shell and k_0 is the ET rate for bare QDs. Experimental plots of the two series of ET rates as a function of ZnS shell thickness can be well fitted by the above equation. The good fit confirms the tunneling of the electron through the ZnS barrier shell. The fitting by the Eq. (1) yields semilogarithmic slopes, β, of 1.1 and 1.4 nm^{-1} for $CuInS_2$/ZnS core/shell QDs 2.5 and 4.0 nm in core diameter, respectively. The slope is comparable to reported one (3.5 nm^{-1}) for CdSe QDs.[5] The value of β for 2.5 nm QDs is less than that in the 4.0 nm QDs. This is because β is dependent on the barrier height for the 1s electron in the $CuInS_2$ core to tunnel into the ZnS shell. Therefore, the 1s electron in the small $CuInS_2$ core is easier to tunnel into the ZnS shell than that in the large core, resulting in smaller factor β.

The eigen function and energy of the electron in $CuInS_2$/ZnS core/shell QDs were calculated to quantify the effect of ZnS shell thickness on the ET rate by modeling them as a particle confined in a spherical well of finite depth.[25,26] The effective mass of electrons is $0.28m_0$ for ZnS.[5] The LUMO levels are −4.1 eV for the $CuInS_2$ core,

−3.1 eV for the ZnS shell,[5] and −0.4 eV for the MPA.[27] We performed the potential well calculation in spherical symmetry for the $CuInS_2$/ZnS core/shell QDs having the same core and ZnS shells differently thick. The diameter of the $CuInS_2$ core was chosen to be 2.5 and 4.0 nm based on TEM images. As shown in Fig. 4, the calculated radial electron densities at the ZnS surface as a function of the ZnS shell thickness are in reasonable agreement with the experimental plots of the shell-thickness-dependent ET rates for the two series of $CuInS_2$/ZnS core/shell QDs. The good agreement with the theoretical calculation confirms the tunneling of the electron through the ZnS barrier shell. On the other hand, this result suggests that optimizing ET efficiency can be realized by controlling the density of the surface states and the ET rate via the change of the shell thickness.

In summary, we have investigated the ET process from $CuInS_2$ core and $CuInS_2$/ZnS core/shell QDs to the porous anatase TiO_2 film. The ET rate reaches 10^7 s^{-1} for different-sized $CuInS_2$ core QDs showing long-lifetime impurity-related emissions. The ET rate as a function of shell thickness was well expressed by an exponential function for the core/shell QDs with core diameters of 2.5 nm and 4.0 nm. This trend is well explained by the electron tunneling calculation of the core/shell QDs. The ET rate is proportional to the existing probability of electrons at the QD surface decreasing exponentially with increasing the shell thickness. These results show the possible ways of optimizing the ET efficiency and QD stability by controlling the core size and shell thickness in QD-based solar cells.

This work was supported by Innovative Research Support Program (Pilot Model) of University of Tsukuba, Japan, Grant-in-Aid for the Scientific Research from the MEXT of Japan (Nos. 23340084 and 23656009) and the program of CAS Hundred Talents and the National Natural Science Foundation of China (Nos. 60976049 and 51102227).

[1]W. U. Huynh, J. J. Dittmer, and A. P. Alivisatos, Science **295**, 2425 (2002).
[2]I. Gur, N. A. Fromer, M. L. Geier, and A. P. Alivisatos, Science **310**, 462 (2005).
[3]R. A. Marcus, J. Chem. Phys. **24**, 966 (1956).
[4]K. Tvrdya, P. A. Frantsuzovc, and P. V. Kamat, Proc. Natl. Acad. Sci. U.S.A. **108**, 29 (2011).
[5]H. Zhu, N. Song, and T. Lian, J. Am. Chem. Soc. **132**, 15038 (2010).
[6]A. Kongkanand, K. Tvrdy, K. Takechi, M. Kuno, and P. V. Kamat, J. Am. Chem. Soc. **130**, 4007 (2008).
[7]D. F. Waton, J. Phys. Chem. Lett. **1**, 2299 (2010).
[8]B. R. Hyun, A. C. Bartnik, J. K. Lee, H. Imoto, L. Sun, J. J. Choi, Y. Chujo, T. Hanrath, C. K. Ober, and F. W. Wise, Nano Lett. **10**, 318 (2010).
[9]J. B. Sambur and B. A. Parkinson, J. Am. Chem. Soc. **132**, 2130 (2010).
[10]Q. Shen, J. Kobayashi, L. J. Diguna, and T. Toyoda, J. Appl. Phys. **103**, 084304 (2008).
[11]L. Li, A. Pandey, D. J. Werder, B. P. Khanal, J. M. Pietryga, and V. I. Klimov, J. Am. Chem. Soc. **133**, 1176 (2011).
[12]H. Zhong, S. S. Lo, T. Mirkovic, Y. Li, Y. Ding, Y. Li, and G. D. Scholes, ACS Nano. **4**, 5253 (2010).
[13]W. S. Song and H. Yang, Appl. Phys. Lett. **100**, 183104 (2012).
[14]B. Chen, H. Zhong, W. Zhang, Z. Tan, Y. Li, C. Yu, T. Zhai, Y. Bando, S. Yang, and B. Zou, Adv. Funct. Mater. **22**, 2081 (2012).
[15]J. Zhang, R. Xie, and W. Yang, Chem. Mater. **23**, 3357 (2011).
[16]W. Zhang and X. Zhong, Inorg. Chem. **50**, 4065 (2011).
[17]X. Tang, W. Cheng, E. S. G. Choo, and J. Xue, Chem. Commun. **47**, 5217 (2011).
[18]X. Yuan, J. Zhao, P. Jing, W. Zhang, H. Li, L. Zhang, X. Zhong, and Y. Masumoto, J. Phys. Chem. C **116**, 11973 (2012).
[19]E. Arici, N. S. Sariciftci, and D. Meissner, Adv. Funct. Mater. **13**, 165 (2003).
[20]See supplementary material at http://dx.doi.org/10.1063/1.4790603 for TEM images as well as the size distribution of the $CuInS_2$/ZnS QDs.
[21]T. A. Heimer, S. T. D'Arcangelis, F. Farzad, J. M. Stipkala, and G. J. Meyer, Inorg. Chem. **35**, 5319 (1996).
[22]All the energy levels in this paper are relative to the vacuum level.
[23]Z. Xu, C. R. Hine, M. M. Maye, Q. Meng, and M. Cotlet, ACS Nano. **6**, 4984 (2012).
[24]K. Tvrdy and P. V. Kamat, J. Phys. Chem. A **113**, 3765 (2009).
[25]J. W. Haus, H. S. Zhou, I. Honma, and H. Komiyama, Phys. Rev. B **47**, 1359 (1993).
[26]D. Schooss, A. Mews, A. Eychmüller, and H. Weller, Phys. Rev. B **49**, 17072 (1994).
[27]Z. Ning, M. Molnár, Y. Chen, P. Friberg, L. Gan, H. Ågren, and Y. Fu, Phys. Chem. Chem. Phys. **13**, 5848 (2011).